

Conceptual Design of a Rocket-Powered Plane And Its Use For Space Tourism

Chul Park*

Department of Aerospace Engineering
Korea Advanced Institute of Science and Technology, Daejeon, Korea 305-701

Kyoung-Ho Kim**

Challenge Space, Inc, Seongnam, Korea 463-420

Abstract

A rocket-powered vehicle is designed conceptually which uses an engine running on methane and oxygen and delivering 10 tons of thrust. The aerodynamic coefficients of the vehicle are taken to be those of the Japan's HOPE-X, and the weight of this vehicle is estimated using a method developed by NASA. The resulting vehicle will be about 9 meters long, 5.8 meters in wing span, weigh about 2 tons empty, carry a maximum of 5.6 tons of propellant, and endure a g-load of 4.5. The craft will be able to carry five passengers, in addition to a pilot, and fly for space tourism between a northern and a southern airport with a maximum g-load varying from 3g to 4g depending on the route flown.

Key Word : Liquid Propellant Rocket, Space Plane, Space Tourism, Reentry, hypersonic aerodynamics

Introduction

In October of 2004, a team led by Burt Rutan and Paul Allen of California succeeded in carrying two passengers to an altitude of 100 km in a rocket-powered plane named SpaceShipOne. Thus an era of space tourism was born. In this report, we ask whether a similar feat can be accomplished in Korea. SpaceShipOne was launched in midair from a carrier aircraft. In Korea, a rocket engine running on methane and oxygen delivering a thrust of 10 tons has been in development for the past several years. We explore here the feasibility of a craft running on this engine, named here Proteus, which takes off from the ground carrying a group of space tourists to an altitude of 100 km. We carry out a conceptual design of the rocket plane, and calculate its flight characteristics. We assume that the aerodynamic characteristics of Proteus are the same as those for a similar Japanese vehicle HOPE under development. Weights of the vehicle are estimated using a method developed in the United States. The flight characteristics are calculated using a three-degrees-of-freedom method. The results indicate that such a vehicle is feasible and will be useful for space tourism.

Vehicle Definition

Engine

Development of a rocket engine operating on liquid oxygen (LOX) and methane (CH₄) was

* Visiting Professor

E-mail : cpark216@kaist.ac.kr TEL : 042-869-3790 FAX : 042-869-3710

** Chief Technical Office

started by Hyundai-MOBIS in the late 1990s. A terrestrial (not flyable) version of the engine, which has a nozzle area ratio of 10 and is fed by an independent propellant feed system, has been in operation for the past several years. Many runs had been made without damage to the engine, thereby demonstrating its reusability. An effort to make a flyable version of this engine incorporating a gas generator and a turbo-pump is being made currently by Challenge and Space, Inc, C&SPACE for short. Based on the data obtained to date, the characteristics of the flying version of the engine are as shown in Table 1. Using the well-known general expressions for a liquid-propellant rocket engine, the thrust values in flight given in Table 1 can be fitted by

$$\text{Thrust (N)} = 3149 \times \text{propellant flow rate (kg/s)} - 0.1437 \times \text{ambient pressure (Pa)}$$

Table 1. Engine characteristics

Item	Value
Thrust chamber diameter	0.1780 m
Nozzle throat diameter	0.1034 m
Nozzle exit diameter	0.4199 m
Divergent section length	0.77 m
Nozzle area ratio	16.5
Thrust chamber pressure	7.2 MPa
Nozzle exit pressure	49.4 kPa
LOX flow rate through engine	24.16 kg/s
CH4 flow rate through engine	8.05 kg/s
LOX flow rate in gas generator	0.5690 kg/s
CH4 flow rate in gas generator	1.1225 kg/s
Sea level thrust without turbine exhaust dump	90.00 kN
Thrust in vacuum without turbine exhaust dump	104.03 kN
Thrust of turbine exhaust dump in vacuum	2.71 kN
Total thrust in vacuum	106.74 kN
Total mass flow rate	33.90 kg/s
Effective specific impulse in vacuum with turbine exhaust	323.1 s

Propellant Tanks

It is desirable that the vehicle has a low drag. To reduce drag, the body must be small, and so the propellant tanks must also be small. This leads to the design of a combined LOX-CH4 tank assembly shown in Fig. 1. As shown in the figure, the two tanks are separated by a relatively thin (5 cm) layer of thermal insulator. The cryogenic temperatures of LOX and liquid CH4 are only 13 degrees C different (96.9 K and 119.9 K for LOX and CH4, respectively). Therefore, when the two tanks are combined as shown in Fig. 1, the heat transfer between the two tanks through the insulator will be small.

The assembly will be constructed of 1.5 mm thick aluminum alloy 5456-H343. This material has a yield strength of 290 MPa. With a safety factor of 1.35, the material will be allowed to be stressed to $290/1.35 = 215$ MPa. This will allow the tank internal pressure to be 2.89 atm at rest. With a maximum g-loading of 4.5g, the bottom side of the LOX tank will be subject to an inertia-caused pressure of 1.40 atm. The allowed 215 MPa will withstand the internal gas pressure of 2.49 atm, with a safety factor of 1.35.

The assembly will be attached to the thrust structure at the bottom flange. The top flange will be attached to the forebody of the vehicle via an elastic pad. The elastic pad will allow thermal shrinkage of the tank assembly when it is cryogenically filled. The cylindrical body of the tank assembly will be sliding inside the round bulkheads of the body structure. The weight of the tank is calculated by multiplying by 1.1 the weight of the 1.5 mm thick aluminum alloy sheet used, in order to account for piping and flange.

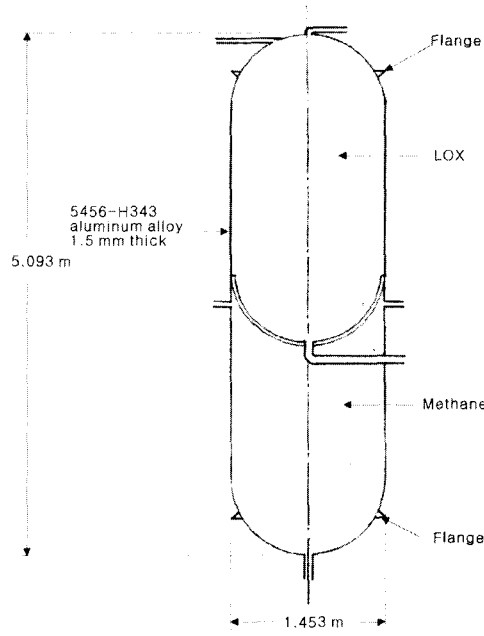


Fig. 1. Schematic of the propellant tank assembly

Vehicle Geometry

The geometrical design of the Proteus vehicle is facilitated greatly by the use of the data for the Japanese HOPE vehicle shown in Fig. 2. HOPE vehicle must carry out an orbital reentry flight, and so its primary design requirement is to minimize the heating rates. This leads to a blunt nose and a large wing sweepback angle. For Proteus vehicle, the heating rate is relatively small. Therefore, the nose can have a smaller radius, and the sweepback angle can be modest. HOPE has no canard, even though canard is known to improve the lift-to-drag ratio, presumably

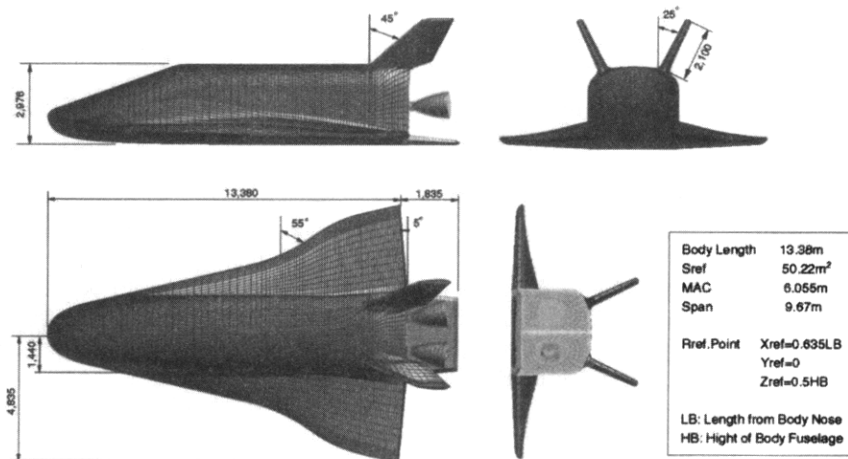


Fig. 2. Geometry of HOPE-X (Ref.1)

Table 2. Specifications of the Proteus vehicles
(a) Dimensions in meters

Item	Value
Body length	8.897
Wing span	5.800
Height	3.483
Forebody length	3.800
Wing tip chord	0.400
Body width	1.683
Body height	1.683
Propellant tank inner diameter	1.550
LOX tank internal length	2.421
CH4 tank internal length	2.613

Table 2. (b) Areas in m²

Item	Value
Wing	6.255
Reference (Wing + area in body)	16.691
Body surface	47.936
Vertical stabilizer with fin	2.520
Canard	0.600
Flap	1.875

Table 2. (c) Volumes in m³

Item	Value
LOX tank	3.713
CH4 tank	3.574
Body	19.37

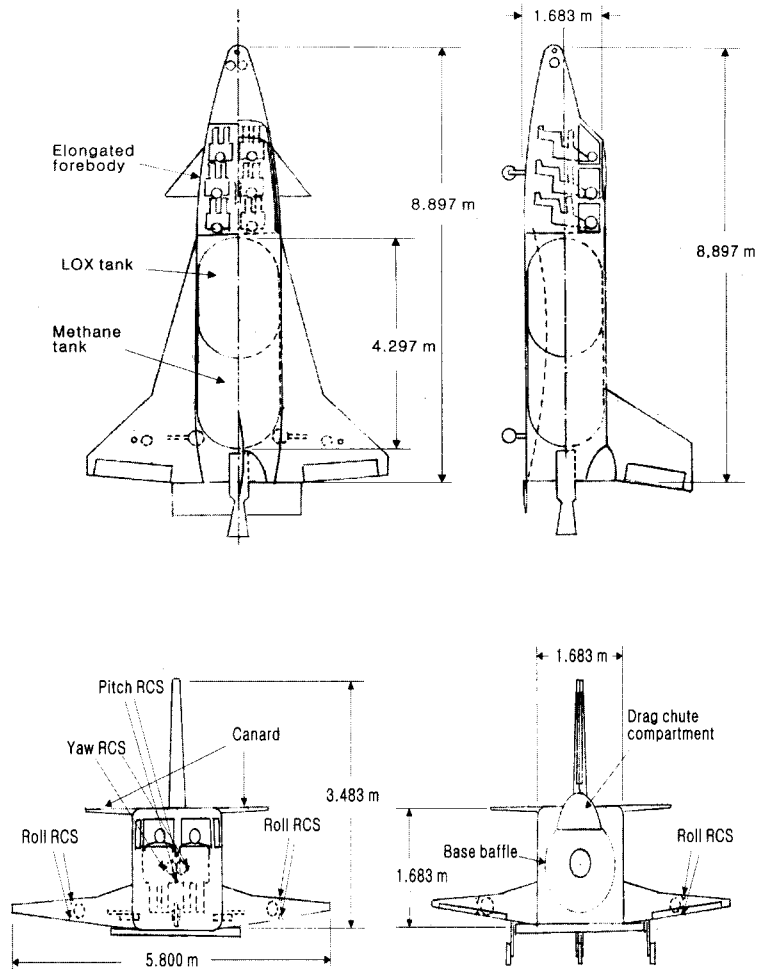


Fig. 3. Geometry of the Proteus vehicle

because the leading edge of the canard is subject to a relatively high heating rate. Because the heating rate is generally low for the Proteus vehicle, it can have a canard. The body fairing seen in HOPE is necessary also for Proteus because it brings the center of pressure (CP) at supersonic Mach numbers forward, and thereby reduces the difference in the CP locations

between the supersonic and subsonic speeds. These considerations lead to a design shown in Fig. 3. The specifications of the vehicle are presented in Tables 2 (a) to (c).

As shown in Fig. 3, the tail region of the fuselage is slightly streamlined to reduce drag. This streamlining reduces the base area, and consequently the base thrust. For the Proteus vehicle, reducing drag is more important than increasing base thrust.

Weights

Weights of the Proteus vehicle are estimated using the Hypersonic Aerospace Sizing Analysis (HASA) method (Ref. 2), with a minor modification, as follows:

1. In the calculation of the weight of avionics, the gross weight in the HASA formula is replaced by empty weight. The resulting value is divided by 2 in order to reflect the miniaturization achievable at present.
2. Weights are not given in the HASA method for tanks that are not an integral part of vehicle structure. Therefore, the tank weight is estimated using the method given above.
3. Weight of drag chute is not given in the HASA method. It is taken to be 2% of the landing weight. This is based on the determination that the weight of the para-wing is 4% of the landing weight (Ref. 3)
4. The weights of the canard and flap, which are not given in the HASA method, are calculated using the formula for the horizontal stabilizer. This is because the forces on these two components will likely be those for the horizontal stabilizer.
5. In the HASA method, the weight of the thermal protection system is estimated from two data sources, orbital reentry vehicles and high speed cruise vehicles. Proteus vehicle is neither, and is typically 20% of the component protected. Compared with those two types of vehicles, thermal load to Proteus is lower. For this reason, the weight of the thermal protection system for a component is estimated here to be 10% of the weight of the component.
6. The Proteus vehicle needs reaction control system engines for attitude control in high altitudes. The weight of these engines is not given in the HASA method. It is arbitrarily assumed in the present work to be 10% of the combined weights of the engine and the propellant tanks.
7. The HASA formulas are for aluminum structures. For any another material, the weight is to be multiplied by a material factor. Using modern composite materials, the weight can be reduced perhaps by 30%. Therefore, the material factor is taken to be 0.7 in the present calculation.
8. The maximum g-loading value needed in the weight calculation is taken to be 4.5g.

The resulting weight values are presented in Tables 3. The mass ratio becomes 3.864, and the delta-V in vacuum becomes 4283 m/sec.

Aerodynamic Characteristics

For the HOPE vehicle, shown in Fig. 2, the drag, lift, and pitching moment coefficients are given in Ref. 2. These coefficient values have been obtained by computational-fluid-dynamics (CFD) calculations, and verified partly by experiments. As Fig. 2 shows, the geometry resembles the geometry of the Proteus vehicle shown in Fig. 3. For this reason, the aerodynamic coefficients for the Proteus vehicle are assumed here to be the same as for the HOPE vehicle. This assumption is believed to lead to a conservative estimation of the coefficients, that is, the assumed drag coefficient will be larger than the true value. This is because the Proteus vehicle is more slender than the HOPE vehicle. The HOPE values are interpolated and extrapolated for use in the

Table 3. Estimated weights in kg

Dry weight				
Engine		154.20		
Structure				
Wing	151.82			
Vertical stabilizer	82.82			
Canard	16.62			
Body	308.05			
Thermal protection	61.45			
Thrust structure	58.45			
Structure subtotal		682.97		
Propellant tanks		126.73		
Subsystems				
Hydraulics	29.83			
Avionics	310.43			
Electrical	81.37			
Subsystem subtotal		421.63		
Landing gear		81.31		
Reaction control system		29.83		
Drag chute		38.90		
Crew + passenger		420.00		
Dry weight subtotal			1955.57	
Propellant				
LOX		4084.44		
CH4		1515.56		
Propellant subtotal			5600.00	
Gross lift-off weight				7555.57

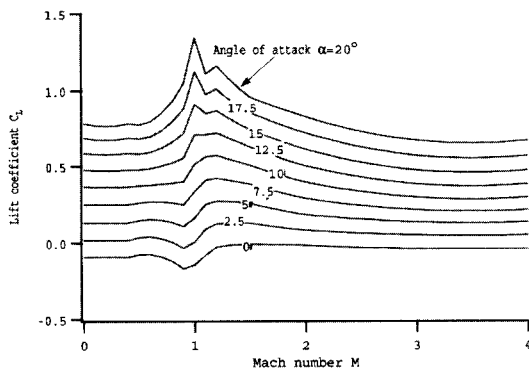


Fig. 4. (a) Lift coefficient

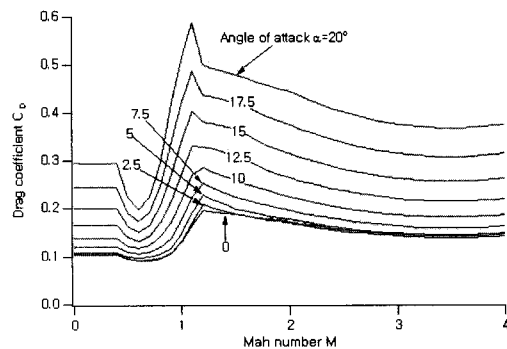


Fig. 4. (b) Drag coefficient

present work. The C_L and C_{Dso} determined are shown as functions of the flight Mach number in Fig. 4(a) and (b).

Heat Transfer Rates

Most of the vehicle will be constructed with composite materials. These composite materials are likely to withstand up to about 400 K. For the components subject to 400 to 600 K, graphite

polyimide will have to be used. Exceptions are the nose dome and the leading edges of the wing, vertical stabilizer, and canard. The radius of the spherical nose dome is envisioned to be 20 cm, and the leading edges of the wing, vertical stabilizer and canard are to have a two-dimensional radius of 2.5 cm. All these leading edges will be swept back 45° .

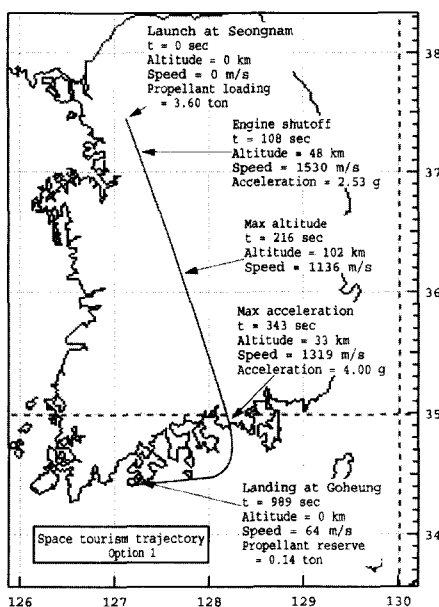
The heat transfer rate to the nose stagnation point is calculated by the well-known Fay-Riddell formula. The heat transfer rates to the leading edges are obtained from the nose stagnation point value by multiplying by the square-root of $20/2.5$, to account for the difference in the radius, dividing by the square-root of 2 to account for the difference between two-dimensional and three-dimensional flows, and multiplying by $\cos(45^\circ)$ to account for the 45° sweepback.

For these highly heated components, carbon phenolic ablator is assumed to be used. The calculated heat transfer rate values are used as inputs to the materials response code KCMA (Korean Charring Materials Ablation) code (Ref. 4). Thermal conductivity and intrinsic density of the material are those in Ref. 4. The initial and final void fractions are taken to be 0.2 and 0.5, and the thickness of the heatshield is assumed to be 1 cm.

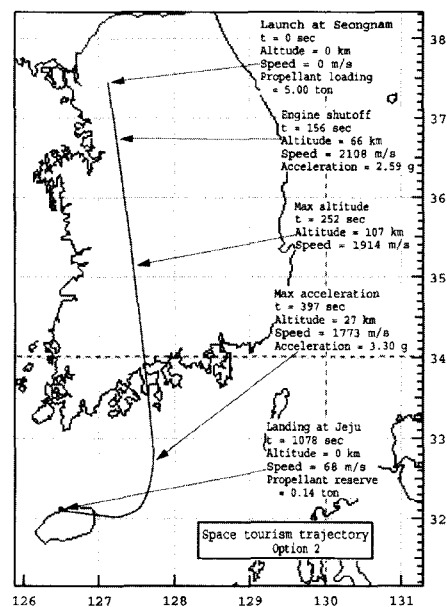
Excluded from consideration is the shock-shock interaction phenomenon. Shock-shock interaction may occur on the leading edges of the wing, vertical stabilizer, or canard. If it occurs, heating rate will be much higher than calculated here. However, the region over which this phenomenon occurs will be relatively small. Over these regions, an ablating material must be used. After each flight, these ablating parts will have to be replaced.

Flight Trajectory Calculation

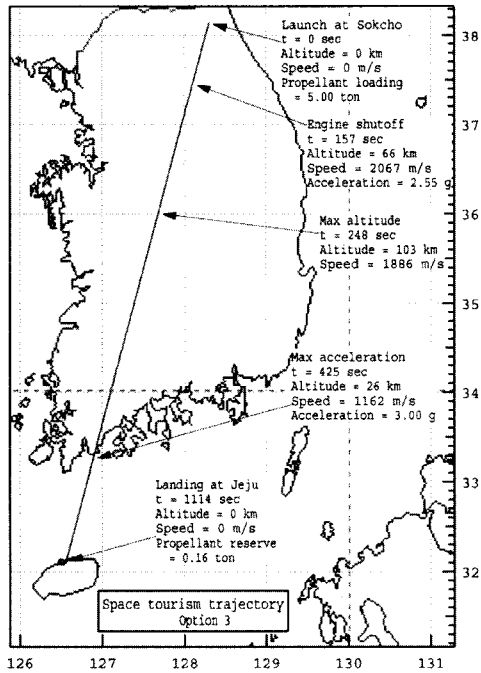
A three-degree-of-freedom trajectory calculation, similar to that made in Ref. 5, was performed using the data given above for possible space tourism missions. Trajectories are shown in Figs. 5(a) to (c) for Options 1 to 3. It is to be noted here that, when the vehicle is flown vertically upward, the highest altitude reached is 373 km. On reentry, this flight reaches a speed of 2,462 m/s and an acceleration of 3.3g. Time of the descending flight to the 20 km altitude is 794 sec. The longest flying distance achievable is 1,017 km.



(a) Option 1



(b) Option 2



(c) Option 3

Fig. 5. Trajectory of space tourism mission

Option 1.

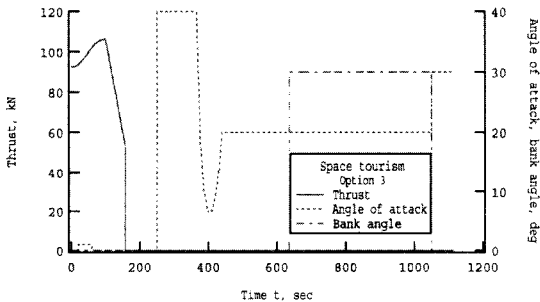
In Option 1, shown in Fig. 5(a), the vehicle is launched at Seongnam and is recovered in Goheung. Seongnam presently has a large airport, and an equally large airport is under construction in Goheung with an intent to be used as a spaceport. The flight path is bent in order to reduce the acceleration, i.e. g-load: by bending the flight path, the downrange distance becomes longer, and therefore the entry angle becomes smaller, which leads to a small g-load. Even with the bent flight path, this mission produces a maximum acceleration of 4g.

Option 2.

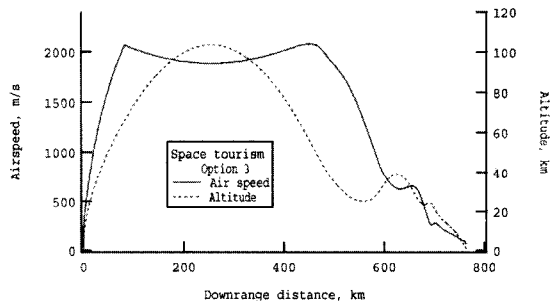
In this Option, shown in Fig. 5(b), the flight path is made longer by landing in Jeju, to reduce the g-load. As a result, the maximum g-load is reduced to 3.3.

Option 3.

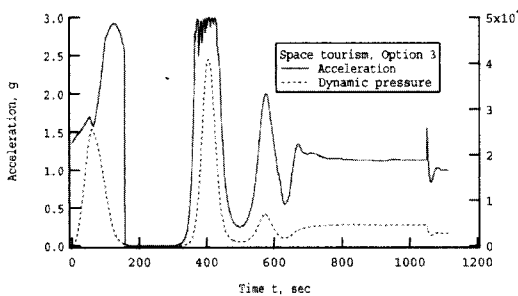
In this Option, shown in Fig. 5(c), launching is made in Sokcho. Because of the long flight path, maximum acceleration is reduced to 3.0g.



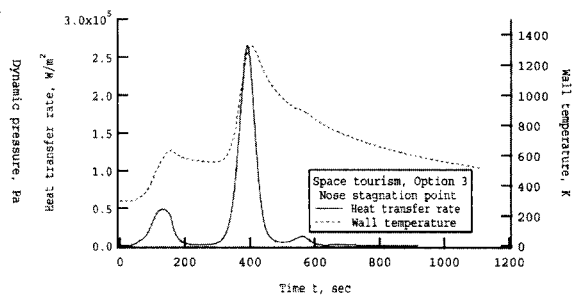
(a) Engine thrust, angle of attack, and bank angle



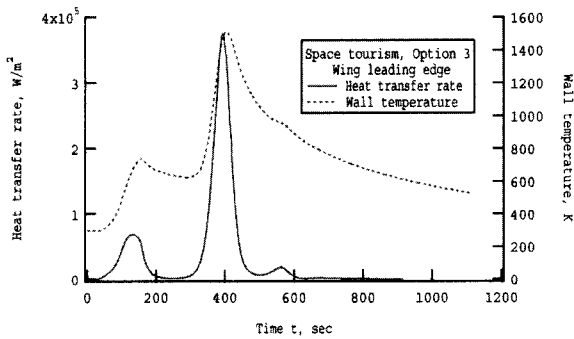
(b) Airspeed and altitude



(c) Acceleration and dynamic pressure



(d) Heat transfer rate and wall temperature at nose stagnation point



(e) Heat transfer rate and wall temperature at wing leading edge

Fig. 6. Flight environment

wing leading edge, and is about 40 W/cm^2 , which is a typical value for the Space Shuttle.

Discussion

The foregoing analysis indicates that the Proteus rocket plane is feasible and will be useful for space tourism purposes. The maximum acceleration encountered is between $3g$ and $4g$. Such acceleration should be tolerable.

The most significant assumption made in the present analysis is that the aerodynamic characteristics of Proteus are the same as those for the Japanese HOPE vehicle. As mentioned, Proteus is slenderer than HOPE and has a canard, and hence will have higher lift-to-drag ratio. Therefore, the true trajectories of Proteus will be more benign in g -loading and heat transfer rates than calculated here.

There will still be several challenges. First, the elevated temperature will make the structural design of this vehicle quite challenging. Aerothermal testing of the highly heated components will be challenging also.

Much of the aerodynamic characteristic determination will have to be made by computational fluid dynamics (CFD). However, certain characteristics will have to be tested experimentally. There are very few, if any, wind tunnels that can produce a flow in the Mach number range from 3 to 5. A new, specially designed shock tunnel, such as that described in Ref. 6, becomes necessary.

Flight testing of the vehicle will require comments. Because this vehicle is manned, it will have to be tested manned from the beginning. As a first step, the vehicle will have to be tested of its gliding and landing characteristics. It will have to be lifted up with a large vehicle, such as an airship, and be released. The very first testing of powered flight will be a big challenge because the vehicle will have no U-turn capability in the beginning. If the vehicle is launched at Seongnam, it will have to fly to Seosan to land, for example.

As pointed out, space tourism flights should preferably made between Sokcho and Jeju. Establishing these bases will be a challenge.

Concluding Remarks

A rocket-powered plane, named Proteus, which uses a methane-oxygen-burning engine, is feasible and could be used to carry five passengers in addition to a pilot, for space tourism. The vehicle will be approximately 60% in length of the Japanese HOPE vehicle, will take off vertically and land horizontally. It will encounter a g -load of 3 and a heat transfer rate of up

The flight environments of Option 3 are shown in Figs. 6(a) to (e). As shown in Fig. 6(a), engine is throttled. Otherwise, acceleration will exceed $3g$. During the reentry, angle of attack is kept at 40° , the maximum allowed, to decelerate gently at high altitudes so as to reduce g -load at lower altitudes. Banking of 30° is executed in the course of gliding toward the landing site. The angle of attack of 30° toward the end is the flaring maneuver for landing. During the flight, air speed reaches $2,000 \text{ m/s}$, altitude of 100 km , acceleration of $3g$, and dynamic pressure of 0.4 atm . The highest heating rate occurs at the

to about 40 W/cm² when operated between Sokcho and Jeju.

References

1. Yamamoto, Y., Yanagihara, M., and Miyazawa, Y., "Pre-flight Analysis of High Speed Flight Demonstrator Phase 2 Vehicle and the Validation of HOPE-X Transonic Aerodynamics", AIAA Paper 2002-0685, January 2002.
2. Harloff, G. J., and Berkowitz, B. M., "HASA-Hypersonic Aerospace Sizing Analysis for the Preliminary Design of Aerospace Vehicles", NASA Contractor Report 182226, November 1988.
3. Sim, A. G., Murray, J. E., Neufeld, D. C., and Redd, R. D., "The Development and Flight Test of a Deployable Precision Landing System for Spacecraft Recovery", NASA Technical Memorandum 4525, September 1993.
4. Ahn, H. K., Park, C., and Sawada, K., "Response of Heatshield Material at Stagnation Point of Pioneer-Venus Probes", *Journal of Thermophysics and Heat Transfer*, Vol. 16, No. 3, July-September 2002, pp. 432-439.
5. Park, C., Menees, G. P., Bowles, J., Lawrence, S., and Davies, C. B., "Bent-Biconic Single Stage-to-Orbit Vehicle Conceptual Study", *Journal of Spacecraft and Rockets*, Vol. 33, No. 4, July-August, 1996, pp. 470-475.
6. Park, C., Chang, K-S., and Jung, Y-G., "Flow Simulation for Mach 3 to 6", 1st International Mach Reflection Symposium cum Shock-Vortex Interaction Workshop, November 1-4, 2004, Jeju, Korea.